

The Changing Hydrogen-Bond Network of Water from the Bulk to the Surface of a Cluster: A Born–Oppenheimer Molecular Dynamics Study

N. Galamba^{*†} and B. J. Costa Cabral^{†,‡}

Grupo de Física-Matemática da Universidade de Lisboa, Av. Prof. Gama Pinto 2, 1649-003 Lisboa, Portugal, and Departamento de Química e Bioquímica, Faculdade de Ciências da Universidade de Lisboa, 1749-016 Lisboa, Portugal

Received September 8, 2008; E-mail: ngalamba@cii.fc.ul.pt

Abstract: The effect of the environment on the properties of water in the bulk and at the surface of a cluster is studied by all-electron Born–Oppenheimer molecular dynamics. The vibrational spectrum of surface and bulk water is interpreted in terms of the molecular orientation and the local changes in the H-bond network of the cluster. Our results show that, in spite of the presence of a surface moiety of “acceptor-only” molecules, the H-bond network is significantly more labile at the surface than in the bulk part of cluster, and single donor–acceptor arrangements are largely dominant at the interface. Further, although surface water molecules depict in average a single H atom protruding into the vapor, molecules exhibit significant orientational freedom. These results explain the *apparently* opposite experimental observations from infrared sum frequency generation and X-ray spectroscopy of the liquid–vapor interface. The dipole moment, intramolecular geometry and surface relaxation are also analyzed at light of the different H-bond regions in the cluster.

I. Introduction

Liquid water is a singular fluid both because of its importance on many physical, chemical and biological processes and for its unique properties related to a labile network of hydrogen bonds (H-bond). A comprehension of the H-bond network is fundamental to explain the changing properties of water resulting from different chemical and physical environments.^{1–4} A drop of water or a relatively large cluster is a prototypical system where different regions are characterized by a specific organization of the H-bond network. Thus, molecules at the surface have similar properties to those at the liquid–vapor planar interface while molecules in the interior of the cluster, the bulk molecules referred here, resemble those of the liquid. A molecular characterization of the surface of aqueous drops is particularly relevant in atmospheric science problems, specifically in the understanding of heterogeneous atmospheric chemical processes.^{5–8} Although the liquid–vapor interface of bulk water

and drops has been the subject of many experimental^{9–15} and molecular dynamics (MD)^{16–24} studies, several issues regarding the dynamics and the microscopic structure of the surface remain unresolved. Here we shall focus on the changes of the H-bond network that stem from surface effects on a cluster of 32 water molecules, and, which are, at the origin of different experimental characterizations of the water liquid–vapor surface. Wilson et al.¹¹ reported the identification of a moiety of “acceptor-only”

[†] Grupo de Física-Matemática da Universidade de Lisboa.

[‡] Faculdade de Ciências da Universidade de Lisboa.

- (1) Stillinger, F. H. *Science* **1980**, *209*, 451–457.
- (2) Luzar, A.; Chandler, D. *Phys. Rev. Lett.* **1996**, *76*, 928.
- (3) Moilanen, D. E.; Levinger, N. E.; Spry, D. B.; Fayer, M. D. *J. Am. Chem. Soc.* **2007**, *129*, 14311.
- (4) Smith, J. D.; Saykally, R. J.; Geissler, P. L. *J. Am. Chem. Soc.* **2007**, *129*, 13847.
- (5) Knipping, E. M.; Lakin, M. J.; Foster, K. L.; Jungwirth, P.; Tobias, D. J.; Gerber, R. B.; Dabdub, D.; Finlayson-Pitts, B. J. *Science* **2000**, *288*, 301.
- (6) Jang, M.; Czoschke, N. M.; Lee, S.; Kamens, R. M. *Science* **2002**, *298*, 814.
- (7) Laskin, A.; Gaspar, D. J.; Wang, W. H.; Hunt, S. W.; Cowin, J. P.; Colson, S. D.; Finlayson-Pitts, B. J. *Science* **2003**, *301*, 340.
- (8) Mundy, C. J.; Kuo, I.-F. W. *Chem. Rev.* **2006**, *106*, 1282–1304.

- (9) Du, Q.; Superfine, R.; Freysz, E.; Shen, Y. R. *Phys. Rev. Lett.* **1993**, *70*, 2313.
- (10) Wilson, K. R.; Rude, B. S.; Catalano, T.; Schaller, R. D.; Tobin, J. G.; Co, D. T.; Saykally, R. J. *J. Phys. Chem. B* **2001**, *105*, 3346.
- (11) Wilson, K. R.; Cavalleri, M.; Rude, B. S.; Schaller, R. D.; Nilsson, A.; Pettersson, L. G. M.; Goldman, N.; Catalano, T.; Bozek, J. D.; Saykally, R. J. *J. Phys.: Condens. Matter* **2002**, *14*, L221.
- (12) Wilson, K. R.; Schaller, R. D.; Co, D. T.; Saykally, R. J.; Rude, B. S.; Catalano, T.; Bozek, J. D. *J. Chem. Phys.* **2002**, *117*, 7738.
- (13) Raymond, A. E.; Tarbuck, T. L.; Brown, M. G.; Richmond, G. L. *J. Phys. Chem. B* **2003**, *107*, 546–556.
- (14) Sovago, M.; Campen, R. K.; Wurple, G. W. H.; Muller, M.; Bakker, H. J.; Bonn, M. *Phys. Rev. Lett.* **2008**, *100*, 173901.
- (15) Liu, D.; Ma, G.; Levering, L. M.; Allen, H. C. *J. Phys. Chem. B* **2004**, *108*, 2252–2260.
- (16) Benjamin, I. *Phys. Rev. Lett.* **1994**, *73*, 2083.
- (17) Vassilev, P.; Hartnig, C.; Koper, M. T. M.; Frechard, F.; van Santen, R. A. *J. Chem. Phys.* **2001**, *115*, 9815.
- (18) Kuo, I.-F. W.; Mundy, C. J. *Science* **2004**, *303*, 658.
- (19) Townsend, R. M.; Rice, S. A. *J. Chem. Phys.* **1990**, *94*, 1991.
- (20) Dang, L. X.; Chang, T.-M. *J. Chem. Phys.* **1997**, *106*, 8149.
- (21) Brodskaya, E. N.; Eriksson, J. C.; Laaksonen, A.; Rusanov, A. I. *J. Colloid Interface Sci.* **1996**, *180*, 86–97.
- (22) Taylor, R. S.; Dang, L. X.; Garrett, B. C. *J. Chem. Phys.* **1996**, *100*, 11720–11725.
- (23) Buch, V. *J. Phys. Chem. B* **2005**, *109*, 17771–17774.
- (24) Kuo, I.-F. W.; Mundy, C. J.; Eggimann, B. L.; McGrath, M. J.; Siepmann, J. I.; Chen, B.; Vieceli, J.; Tobias, D. J. *J. Phys. Chem. B* **2006**, *110*.

water molecules from X-ray experiments at the water surface. This observation engenders the possibility that a significant fraction of surface water molecules have two free hydrogen atoms protruding into the vapor phase. This hypothesis however finds no support from the interpretation of the experimental vibrational spectrum^{9,13,16,25} of surface water from which, Du et al.⁹ predicted more than 20% of surface water molecules with a single H atom dangling away from the surface with an angle of 38° with the surface normal. Moreover, the authors⁹ argued that if both H atoms were free, then, two sharp peaks would appear in the vibrational spectrum. *Ab initio* MD¹⁸ of the liquid–vapor interface also predicted the existence of a surface “acceptor-only” moiety. A profounder molecular characterization of the liquid–vapor interface is therefore in need to explain what prevents surface water “acceptor-only” molecules from displaying symmetric and antisymmetric vibrational peaks.

Another related issue concerns surface relaxation, which is characterized by a larger intermolecular O–O distance between surface molecules. Experimental^{10,12} X-ray absorption studies predicted a 5.9% increase of the O–O separation. Kuo and Mundy¹⁸ further observed surface relaxation from Voronoi volume analysis. Recently, however, Cappa et al.²⁶ presented evidence that these^{10–12} previous experimental results concerning surface relaxation, and the finding of an “acceptor-only” moiety could have resulted from experimental artifacts, and the X-ray absorption spectrum of the liquid–vapor interface is actually similar to that of liquid water. At light of these different observations we present here results for a cluster, for which surface effects are dominant, allowing a comparison between the H-bond network in a spherical surface and that of the liquid–vapor planar interface. The method chosen to carry out this study was, density functional theory^{27,28} based, all-electron Born–Oppenheimer molecular dynamics (BOMD).

II. Methods

The present BOMD was carried out in the microcanonical ensemble for a cluster with 32 water molecules using a MD code developed by the authors coupled to the program Gaussian 03.²⁹ The equations of motion were integrated with a Verlet “leap-frog” algorithm and a time-step (Δt) of 0.9 fs. The electronic energy and forces were calculated with the Perdew–Burke–Ernzerhof³⁰ generalized gradient approximation (PBE-GGA) exchange–correlation (XC) functional and a 6–31+G(d,p) basis set with a tolerance of 10^{-8} Ha in the energy. The choice of the functional and time-step in the present study was driven by results of preliminary MD simulations of clusters with 8 water molecules at room temperature, where different XC functionals and time-steps were examined. The choice of the PBE-GGA functional resulted from the fact that vaporization of the cluster was not observed for different, nonequilibrated, starting configurations. On the other hand, due the computational cost of all-electron BOMD, the choice of a time-step slightly larger than the typical value of 0.5 fs commonly used in simulations of liquid water, is desirable. The combination of the Verlet “leap-frog” algorithm with a time-step of 0.9 fs, results in conservation of the total energy and linear momentum within the limits of accuracy of the present calculations. The water molecules were

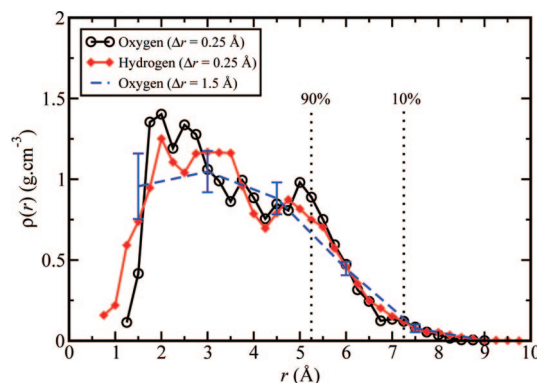


Figure 1. Water molecules oxygen and hydrogen (divided by two) atoms radial density profiles. The dashed line represents the oxygen density profile calculated for concentric layers of 1.5 Å to estimate the density ($1.0 \text{ g}\cdot\text{cm}^{-3}$) in the liquid region. The error bars are the standard deviation at each 1.5 Å layer.

given, at time zero, the experimental geometry³¹ ($r_{\text{O-H}} = 0.957 \text{ \AA}$, $\alpha_{\text{HOH}} = 104.5^\circ$), of the isolated monomer, and were displayed on the surface of two concentric spheres, 2.91 Å apart, around a central molecule. The first sphere surface accommodated 6 molecules and 25 water molecules were spread at the surface of the second. The molecules were then randomly rotated between 0 and 2π and the cluster was equilibrated for 3.8 ps followed by a production stage of 7.1 ps. The atomic velocities were scaled for a temperature of 300 K during the first 1.35 ps of equilibration. The profiles reported herein, for the 7.1 ps run, were also calculated at different time blocks of ~ 1.75 ps of the equilibration and production stages to ensure that 3.8 ps were enough for the cluster to attain equilibrium and to monitor property changes within different periods of the simulation. The average temperature of the cluster was $317 \pm 24 \text{ K}$.

The dipole moment of the water molecules was calculated from natural population analysis³² (NPA) and Mulliken³³ atomic charges. Although deficient for a quantitative analysis of the dipole moment of the isolated monomer these methods do not suffer from the problems of electrostatic potential methods for large molecules or clusters.³⁴ The NPA method highly overestimates the dipole moment of the water monomer. For the PBE/6–31+G(d,p) water monomer geometry ($r_{\text{O-H}} = 0.973 \text{ \AA}$, $\alpha_{\text{HOH}} = 104.9^\circ$) the dipole moment of the isolated water molecule is $\mu_{\text{NPA}} = 2.8 \text{ D}$ to be compared with the experimental 1.855 D.³⁵ A significantly lower value is obtained from Mulliken population analysis, $\mu_{\text{Mulliken}} = 2.0 \text{ D}$, although this value is more sensitive to the size of the basis set.³⁴ More importantly, however, for the purposes of the present study, is to understand whether or not the chosen population methods have the ability to correctly capture polarization effects when we move from the surface to the interior of the cluster.

The H-bond analysis was based on the following geometric definition:² $r_{\text{OO}} < 3.5 \text{ \AA}$ and $\phi_{\text{HOO}} < 30^\circ$, where r_{OO} is the distance between the donor and acceptor oxygen atoms and ϕ_{HOO} is the angle between the intramolecular O–H bond and r_{OO} . The radial profiles presented herein were calculated by dividing the cluster in concentric spherical layers of thickness, $\Delta r = 0.25 \text{ \AA}$.

III. Results and Discussion

Figures 1 and 2 depict the density radial profile of oxygen (O) and hydrogen (H) atoms and the number of donor/acceptor

(25) Morita, A.; Hynes, J. T. *Chem. Phys.* **2000**, *258*, 371–390.
 (26) Cappa, C. D.; Smith, J. D.; Wilson, K. R.; Saykally, R. J. *J. Phys.: Condens. Matter* **2008**, *20*, 205105.
 (27) Hohenberg, P.; Kohn, W. *Phys. Rev. B* **1964**, *136*, B864.
 (28) Kohn, W.; Sham, L. J. *Phys. Rev. A* **1965**, *140*, A1133.
 (29) Frisch, M. J.; et al.; *Gaussian 03*, Revision C.02; Gaussian, Inc.: Wallingford, CT, 2004.
 (30) Perdew, J. P.; Burke, K.; Ernzerhof, M. *Phys. Rev. Lett.* **1996**, *77*, 3865.

(31) Benedict, W. S.; Gailar, N.; Plyer, E. K. *J. Chem. Phys.* **1956**, *24*, 1139.
 (32) Reed, A. E.; Weinstock, R. B.; Weinhold, F. *J. Chem. Phys.* **1985**, *83*, 735.
 (33) Mulliken, R. S. *J. Chem. Phys.* **1955**, *23*, 1833.
 (34) Zipse, H.; Martin, F. J. *Comput. Chem.* **2005**, *26*, 97.
 (35) Clough, S. A.; Beers, Y.; Klein, G. P.; Rothman, L. S. *J. Chem. Phys.* **1973**, *59*, 2254.

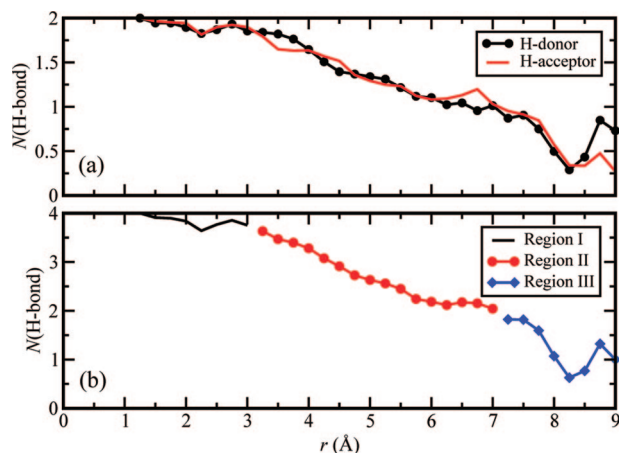


Figure 2. (a) Number of H-bond donor and acceptor radial profiles. (b) Definition of different H-bond regions based on the total number of H-bonds.

H-bond profiles, respectively. We distinguish 3 H-bond regions, based on the radial average number of H-bonds: a bulk, almost tetrahedral, region (I) at $r \leq 3$ Å, a surface-vapor region (III) where in average molecules have less than two H-bonds, at $r > 7$ Å, and a larger in-between region (II) where molecules have either one or two donor and acceptor H-bonds (see Figure 2). These regions are to be distinguished from the bulk-surface definition based on the density changes of water. The region where the density changes between 90% and 10% of the bulk density is commonly applied to define the liquid–vapor interface. This region was found here to be around, $5.25 \text{ \AA} < r < 7.25 \text{ \AA}$, (see Figure 1). The density in the liquid region (1.0 g.cm^{-3}) of the cluster was obtained through the fitting of a hyperbolic tangent function^{36,37} to the density profile of O ($\Delta r = 1.5 \text{ \AA}$).

The average number of H-bonds in the H-bond region I is approximately 3.85, which is in good agreement with the conventional description of liquid water with a nearly four H-bond tetrahedral local structure.^{38–41} This means that despite of the small size of the cluster there is a region where molecules have a similar coordination to that typically found in liquid water. We note, however, that the structure of liquid water is presently the subject of intense debate.^{41–46} Wernet et al.⁴⁶ suggested, from the interpretation of X-ray absorption spectra,

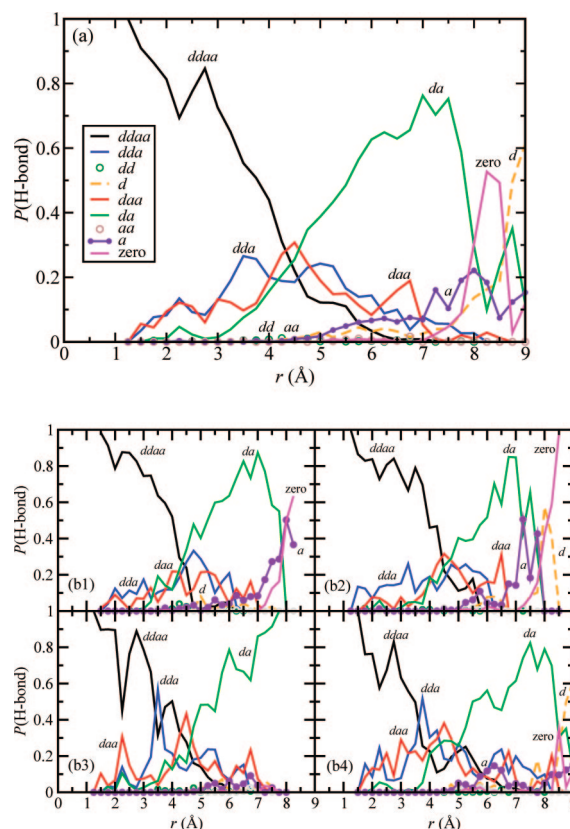


Figure 3. (a) Water H-bond coordination type molecular fraction radial profile; d and a stand for H-bond donor and acceptor water molecules, respectively. (b) H-bond profile obtained from the first (b1), second (b2), third (b3), and fourth (b4) periods of 1.75 ps of the simulation. The zero refers to molecules without any H-bond.

an alternative picture of the structure of liquid water where a majority of water molecules experience a distorted and asymmetric H-bonding environment with each molecule forming a single strong donor and a single strong acceptor H-bond. More recently Tokushima et al.⁴⁵ proposed that liquid water is characterized by tetrahedral and strongly distorted H-bond species in a (1:2) ratio. The results presented here do not support this view and keep with the observations of other experimental studies as well as quantum calculations and DFT and classical force field MD simulations.

A more detailed ($\Delta r = 0.25 \text{ \AA}$) examination of the density profiles reveals that the H density profile extends over larger distances in both H-bond regions, I and III, which suggests that at least a single H atom is oriented toward the center of mass and outside the cluster surface, respectively. Additionally we encounter a $\sim 0.5 \text{ \AA}$ void around the center of mass of the cluster. We must stress that the radial profiles have a poor statistics at small r and large fluctuations of the density profile in the inner layers are usually observed, even for large drops.^{21,37} This is inherent to the calculation in the sense that the interior layers have a smaller volume and averages are therefore taken over smaller populations.³⁷ Nonetheless, we shall see that the O and H density differences observed in the H-bond region I are related to the specific molecular orientation adopted by the water molecules.

Figure 3a displays a radial profile of the H-bond network, which provides local quantitative information on the fraction of water molecules that adopt a specific type of H-bond coordination of the possible, single and double, donor (d) acceptor (a), combinations. A double donor-double acceptor

- (36) Allen, M. P.; Tildesley, D. J. *Computer Simulations of Liquids*; Clarendon Press: Oxford, 1987.
- (37) Thompson, S. M.; Gubbins, K. E.; Walton, J. P. R. B.; Chantry, R. A. R.; Rowlinson, J. S. *J. Chem. Phys.* **1984**, *81*, 530–542.
- (38) Bukowski, R.; Szalewicz, K.; Groenenboom, G. C.; van der Avoird, A. *Science* **2007**, *315*, 1249–1252.
- (39) Prendergast, D.; Galli, G. *Phys. Rev. Lett.* **2006**, *96*, 215502.
- (40) Hakala, M.; Nygård, K.; Manninen, S.; Huotari, S.; Buslaps, T.; Nilsson, A.; Pettersson, L. G. M.; Hämmäläinen, K. *J. Chem. Phys.* **2006**, *125*, 084504.
- (41) Smith, J. D.; Cappa, C. D.; Wilson, K. R.; Messer, B. M.; Cohen, R. C.; Saykally, R. J. *Science* **2004**, *306*, 851–853.
- (42) Head-Gordon, T.; Johnson, M. E. *Proc. Natl. Acad. Sci. U.S.A.* **2006**, *103*, 7973–7977.
- (43) Hermann, A.; Schmidt, W. G.; Schwerdtfeger, P. *Phys. Rev. Lett.* **2008**, *100*.
- (44) Leetmaa, M.; Wikfeldt, K. T.; Ljungberg, M. P.; Odelius, M.; Swenson, J.; Nilsson, A.; Pettersson, L. G. M. *J. Chem. Phys.* **2008**, *129*.
- (45) Tokushima, T.; Harada, Y.; Takahashi, O.; Senba, Y.; Ohashi, H.; Pettersson, L. G. M.; Nilsson, A.; Shin, S. *Chem. Phys. Lett.* **2008**, *460*, 387–400.
- (46) Wernet, P.; Nordlund, D.; Bergmann, U.; Cavalleri, M.; Odelius, M.; Ogasawara, H.; Naslund, L. A.; Hirsch, T. K.; Ojamae, L.; Glatzel, P.; Pettersson, L. G. M.; Nilsson, A. *Science* **2004**, *304*, 995–999.

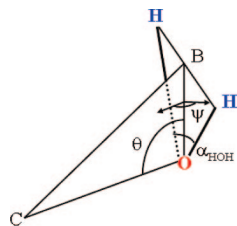


Figure 4. Angles θ (0° – 180°) and ψ (0° – 90°) (dihedral) used to study water molecules orientation. C represents the center of mass of the cluster and OB is the intramolecular angle, α_{HOH} , bisector. The angle ψ is made to vary between (0° – 90°) due to the fact that the atoms of H are indistinguishable. The figure depicts both, θ and ψ with an angle of 90° . For $\theta = 90^\circ$ and $\psi = 0^\circ$ the water molecule plane lies perpendicular to the surface; if $\theta = 90^\circ$ and $\psi = 90^\circ$ the water molecule plane lies in the interface.

(*ddaa*) arrangement is predominant in the bulk region of the cluster until about 4.5 Å. At longer distances from the center of mass, where surface effects are dominant, single donor–single acceptor (*da*) coordination increases until around 7 Å. The decrease of (*da*) for $r > 7$ Å is concomitant with the increase of free molecules (zero) and single acceptor-only (*a*) and single donor-only (*d*) H-bond arrangements. Arrangements of the type double donor-only (*dd*) and double acceptor-only (*aa*), are not abundant in any region of the cluster. Figure 3b shows the H-bond profiles obtained by dividing the MD time (7.1 ps) in four blocks of ~ 1.75 ps. It can be seen that the H-bond populations (*ddaa*, *daa*, *add* and *da*) in the H-bond regions I and II are almost constant in the different time-blocks. However, in the outermost H-bond region III of the cluster large fluctuations take place and the populations of *d*, *a*, *da* and zero H-bonds constantly change. For example in Figure 3b we can see that the fraction of molecules with *d*, *a* and zero H-bonds is negligible and almost all the molecules exhibit single donor–acceptor (*da*) coordination. On the other hand in Figure 4b the cluster slightly expanded due to the increase of *d*, *a* and zero H-bond moieties. As discussed by Wilson et al.¹¹ these moieties may play a significant part on water evaporation and condensation mechanisms. Hence, a mechanism whereby a captured molecule forms two H-bonds could be less probable than one where a single H-bond (*d* or *a*) formation occurs.

Examination of water molecules orientation relative to the surface normal was carried out by calculating the two angles¹⁹ (θ and ψ) defined in Figure 4. θ is the angle between the intramolecular angle, α_{HOH} , bisector (OB) and the vector (OC) normal to the surface, and ψ is the dihedral between the plane of the water molecule and the plane COB. Figure 5 shows the angle distributions and the corresponding radial profiles of θ and ψ for the three H-bond regions of Figure 2. As it may be seen from Figure 5, large angle distributions, $P(\theta)$ and $P(\psi)$, characterize the water molecules orientation, especially at the H-bond regions II and III. This absence of a well-defined orientation indicates that molecules possess significant rotational freedom which is explained by the reduced H-bond coordination environment observed as the surface of the cluster is approached. Nonetheless, the water molecules adopt a preferential orientation in the H-bond regions II and III, where a single atom of H protrudes into the vapor ($\theta \sim 70^\circ$ – 110°), without a single well-defined angle (ψ), relative to the surface normal. This view is therefore different from that, which attributes a well-defined orientation to surface water,⁹ and also from the possibility of a significant fraction of water molecules at the liquid–vapor interface to depict two free H atoms dangling away from the surface.

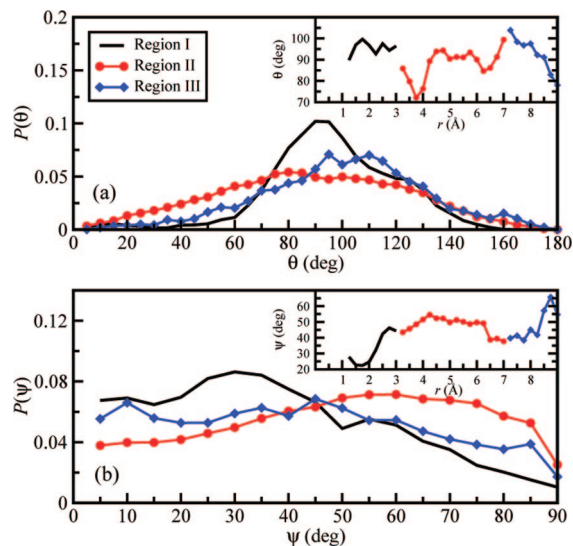


Figure 5. Orientation angles distributions, (a) $P(\theta)$ and (b) $P(\psi)$ for the three H-bond regions. (Insets) Radial profiles of the water orientation angles, θ and ψ .

Interestingly, a minimum and maximum of ψ at $\sim 20^\circ$ and $\sim 50^\circ$ take place in the H-bond region I (see inset of Figure 5(b)), denoting a change of orientation, which explain the O and H local density differences observed in this region (see Figure 1). On the other hand the 0.5 Å void results from intermolecular H repulsions since molecules in the innermost layers have one H atom pointing ($\theta \approx 95^\circ$ and $\psi \approx 20$ – 30°) toward the center of mass of the cluster.

The vibrational spectrum of the water cluster and that of bulk and surface water molecules was calculated through Fourier transform of the H velocity autocorrelation functions. This method, replaces the macroscopic dipole moment (or its time derivative) correlation function by the H velocity autocorrelation function and involves the neglect of both intra and intermolecular cross terms in the computed time correlation function.^{16,47–49} Although this affects the intensities, the position of the intramolecular bending and stretching peaks in the power spectrum, remains unchanged.⁴⁷ A rigorous computation of the vibrational spectrum of water even at room temperature requires however a quantum description of the H atoms.^{16,48}

There is some ambiguity in the choice of bulk and surface molecules within the cluster since there are not molecules at all times in the interior or at the surface of the cluster. The bulk and surface water vibrational spectra (see Figure 6) were calculated here, respectively, for 3 and 4 molecules, and a period of 5 ps. During this time the molecules occupied, respectively the H-bond regions I and III of Figure 2. The reason to choose molecules in the H-bond region III to characterize the vibrational spectrum of surface water, rather than the H-bond region II or the 10%–90% region, is that, it is in this region (see Figure 3) that the population of zero and single acceptor-only molecules is more significant. The need to isolate a time subinterval of our simulation, to characterize molecules in the interior and at the surface of the cluster limits the maximum delay-time to compute the H velocity autocorrelation functions to this

(47) Marti, J.; Guardia, E.; Padro, J. A. *J. Chem. Phys.* **1994**, *101*, 10883–10891.

(48) Lobaugh, J.; Voth, G. A. *J. Chem. Phys.* **1997**, *106*, 2400–2410.

(49) McQuarrie, D. A. *Statistical Mechanics*; Harper & Row: New York, 1976.

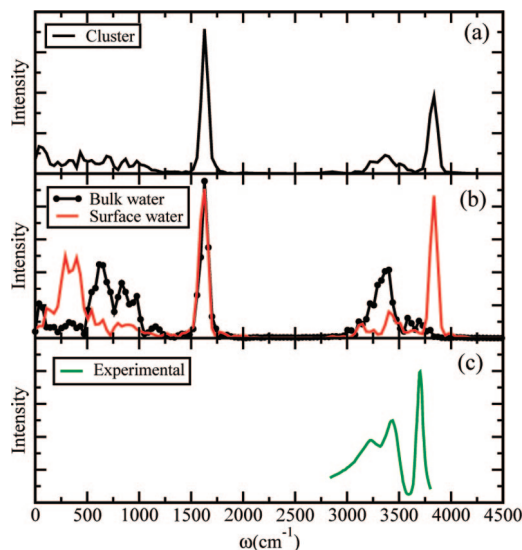


Figure 6. (a) Vibrational spectrum of the water cluster (32 molecules). (b) Vibrational spectrum of bulk (3 molecules) and surface (4 molecules) water molecules. (c) Water liquid–vapor experimental VSGF spectrum of Due et al.⁹

subinterval. In the present study the H velocity autocorrelation functions were calculated for ~ 0.9 ps (1024 points).

Vibrational sum frequency generation (VSGF)^{9,13} of the liquid water interface revealed a sharp peak at ~ 3700 cm⁻¹ assigned to an unperturbed O–H vibration and a shoulder at ~ 3200 cm⁻¹ of the band at 3400 cm⁻¹ of liquid water (see Figure 6c). Although the high frequency peak interpretation is generally accepted, the double-peak (3200 and 3400 cm⁻¹) assignment has been much debated.^{9,13–15,23,25} These peaks have been primarily assigned to the different H-bond environments at the interface. Recently, Sovago et al.¹⁴ presented experimental evidence that the double-peaked structure of interfacial (heavy) water originates from vibrational coupling between the stretch and bending overtone, rather than from different H-bond arrangements. The interpretation of this band is beyond the scope of our analysis and its assignment does not collide with any of our observations.

The simulated spectrum of bulk water shown in Figure 6b depict a band (500 – 1000 cm⁻¹) in the far-infrared (IR) region corresponding to water molecules hindered rotations (librations), a sharp peak around 1629 cm⁻¹, which can be assigned to bending, and a larger band centered at ~ 3402 cm⁻¹ associated to stretching vibrations. The experimental bands assigned to bending and stretching vibrations appear around 1650 cm⁻¹ and 3400 cm⁻¹, respectively, in the spectrum of liquid water.⁵⁰ For the computed spectrum of surface water (see Figure 6b) the band corresponding to the water librational modes is red-shifted (100 – 500 cm⁻¹) reflecting the fact that the surface molecules sampled have significant rotational freedom. The bending band frequency is not changed and the stretching broad peak is now splitted into a sharp peak at 3837 cm⁻¹, the bulk water band at 3402 cm⁻¹, and a low intensity peak around 3149 cm⁻¹ with a shoulder at ~ 3258 cm⁻¹. The mid-IR region in the computed spectrum of the whole cluster displayed in Figure 6a resembles that of surface water, denoting that surface effects are predominant in our cluster. We can therefore assign our peaks to the vibrational spectrum of the liquid–vapor planar interface, the only significant difference being a blue shift of the free O–H

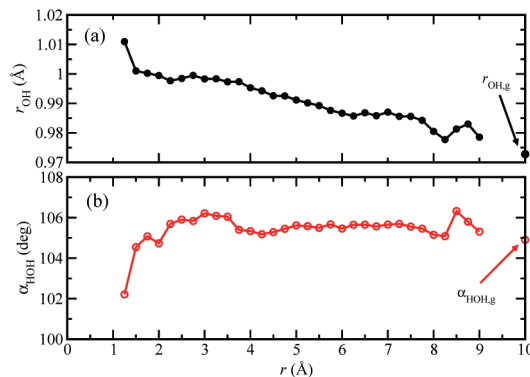


Figure 7. (a) Intramolecular OH bond length, r_{OH} , profile. (b) Intramolecular angle, α_{HOH} , profile. The arrows signal the geometry of the gas (g) phase PBE/6–31+G(d,p) water molecule. Experimental values for r_{OH} and α_{HOH} for liquid (heavy) water are, respectively, 0.970 Å and 106.6° .⁶²

stretching vibration (from ~ 3700 to ~ 3837 cm⁻¹). The origin of this blue shift, relative to the liquid–vapor planar surface, is likely due to the present XC functional/basis-set combination, rather than the spherical geometry of the cluster surface. We note that classical¹⁶ and *ab initio*¹⁸ MD of the planar interface also revealed spectra similar to VSGF.^{9,13} The fact that the simulated vibrational spectrum for surface water exhibits a single stretching sharp peak (~ 3837 cm⁻¹) further supports, therefore, the idea that the second free H atom is still an active partner in the forming/breaking H-bond network dynamics of surface water. Hence, the computed vibrational spectrum of surface water reflects only the presence of the predominant species (*da*), in opposition to depicting two sharp peaks corresponding to the symmetric (3657 cm⁻¹)⁵⁰ and antisymmetric (3756 cm⁻¹)⁵⁰ peaks of the isolated monomer, even though our H-bond profiles reveal the presence of molecules with zero H-bonds and single acceptor-only (*a*) arrangements. In spite of the recent X-ray absorption experimental results reported by Cappa et al.,²⁶ which show that the electronic structure of the water interface cannot be distinguished from that of the liquid, it appears plausible, therefore, that surface water has an “acceptor-only” component which cannot be traced also through VSGF.

We shall turn attention now to the geometrical deformations and its effect on the dipole moment of water molecules caused by the distinct environments experienced by water molecules in the cluster. As may be seen from Figure 7 the intramolecular angle, α_{HOH} , increases throughout the H-bond region I up to a maximum $\sim 106.6^\circ$ and has an approximate constant value $\sim 105^\circ$ in the other H-bond regions. This behavior is not followed by r_{OH} , which increases almost linearly from the surface down to the H-bond region I. The large fluctuations at $r > 8.25$ Å are associated to the expansion of the cluster observed in Figure 3b leading to a poor statistics in this small region (see also Figure 2). Our results show that water molecules in the bulk region have elongated OH bonds causing α_{HOH} to decrease due to weaker intramolecular H repulsion, in agreement with previous classical MD observations.¹⁹ For the outer H-bond regions α_{HOH} is less sensitive to the changes in r_{OH} .

In Figure 8 we compare the dipole moment radial profile calculated using NPA, and Mulliken atomic charges. We also report the dipole moment, denoted here by $\mu(r_{OH}, \alpha_{HOH})$, calculated for arbitrary atomic charges, chosen to be $q_O = -0.6515 e$ for all molecules in the cluster. This value reproduces the experimental dipole moment of the isolated monomer ($1.855 D^{35}$) for the PBE/6–31+G(d,p) geometry. We observe that molecules at the surface of the cluster have a dipole moment

(50) Maréchal, Y. *J. Chem. Phys.* **1991**, *95*, 5565.

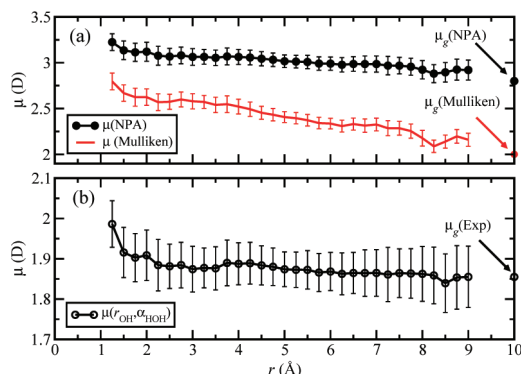


Figure 8. (a) Dipole moment (in Debyes (D)) radial profile obtained from NPA and Mulliken atomic charges. (b) Dipole moment profile calculated using equal charges for all molecules. The error bars are the standard deviations of the radial time averages. The arrows signal the dipole moment of the gas (g) phase PBE/6-31+G(d,p) water molecule calculated with the different charges. The experimental dipole moment of liquid water is 2.9 ± 0.6 D.⁵¹

(see Figure 8(a)) only slightly higher than the corresponding gas phase values, a trend already depicted in MD liquid–vapor studies of water.^{18,20,24} Moreover, the dipole moment calculated from NPA charges is significantly less sensitive to polarization effects than that of Mulliken charges. The slight increase of $\mu(r_{\text{OH}}, \alpha_{\text{HOH}})$ from the surface up to ~ 4 Å reflects the elongated intramolecular OH bond of molecules in the bulk relative to those at the surface of the cluster. The maximum and minimum of α_{HOH} in the innermost layers of the cluster cause the additional decrease and enhancement of the dipole moment. Nonetheless, within the errors of our analysis the dipole moment appears to be insensitive to the geometry deformations of the water molecules in the H-bond network. The dipole moment enhancement of the water molecule in the liquid^{51–57} and clusters,^{58–60} relative to that of the isolated monomer, resulting from polarization effects is still not fully understood and values between 2.5–3.1 D for the dipole moment of liquid water have been reported.

Finally, a characterization of the cluster in terms of surface relaxation was carried out through the calculation of the intermolecular O–O distance profile of water molecules H-bonded, $r_{\text{OO}}(\text{H-bond})$ (see Figure 9). As it may be seen from Figure 9 there is a leap of the O–O distance inside region I, where the water molecules population is significantly lower, followed by a slight increase ($\sim 1\%$) until the end of the H-bond region II. In the H-bond region III the fluctuations are very large as expected. Because of the statistics of our MD it is not possible to ascertain about the degree of relaxation of the surface of the water cluster in a quantitative manner. Nonetheless, if we neglect the two innermost layers in region I and the region III, a significantly lower relaxation appears to take place, compared to the experimental¹¹ 5.9%, when

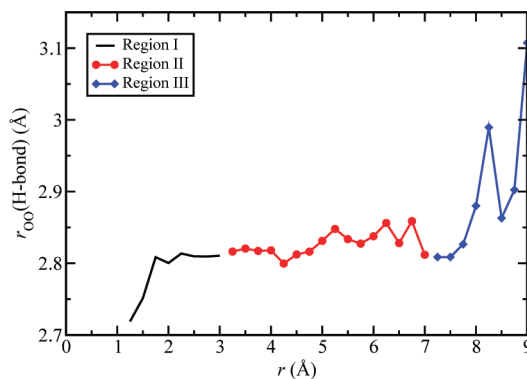


Figure 9. Radial profile of the intermolecular O–O distance between water molecules H-bonded.

passing from the H-bond region I to the H-bond region II. We recall, however, that this experimental value has been recently questioned by Cappa et al.,²⁶ although in this study, surface relaxation was not directly addressed. On the other hand, a contraction of the O–O distance, rather than the expansion observed from *ab initio* MD,^{18,24} has been predicted from classical molecular dynamics studies of different empirical interaction potentials for water.²⁴ A recent study on water clusters using the polarizable force field AMOEBA, however, also predicts longer O–O distances at the cluster surface than in the bulk.⁶¹ Our results indicate that even though a surface relaxation takes place, this effect, is not pronounced.

IV. Concluding Remarks

The relationship between the local H-bond network with the properties of water in a small cluster was addressed through all-electron Born–Oppenheimer molecular dynamics. Remarkably, in spite of the small size of the cluster, it was possible to unambiguously observe a change in the computed vibrational spectrum as well as on the dipole moment and geometry of water molecules, as the surface of the cluster is approached, similar to those observed for the liquid–vapor planar interface relative to liquid water. Our results strongly indicate that the water molecules at the surface of the cluster are characterized by significant orientational freedom. Hence, although a population of H-bond “acceptor-only” water molecules is observed at the surface, the two free H atoms do not point preferentially away from the liquid surface. Instead, we observe that these populations are extremely labile competing with single donor–acceptor (*da*) and single donor-only (*d*) H-bond arrangements, where a single H-bond dangles. The surface of the cluster is, therefore, largely dominated by single donor–acceptor arrangements, which explains the single-well defined stretching peak in the vibrational spectrum of the liquid–vapor interface of water, assigned to a free O–H vibration. Finally, regarding surface relaxation of water, although not fully conclusive, our results suggest that a slight expansion, rather than a contraction of the O–O distance, takes place as the surface of the cluster is approached.

Supporting Information Available: Complete ref 29. This material is available free of charge via the Internet at <http://pubs.acs.org>.

JA807111Y

- (51) Badyal, Y. S.; Saboungi, M.-L.; Price, D. L.; Shastri, S. D.; Haefner, D. R.; Soper, A. K. *J. Chem. Phys.* **2000**, *112*, 9206.
 (52) McGrath, M. J.; Siepmann, J. I.; Kuo, I.-F. W.; Mundy, C. J. *Mol. Phys.* **2007**, *105*, 1411.
 (53) Silvestrelli, P. L.; Parrinello, M. *Phys. Rev. Lett.* **1999**, *82*, 3308.
 (54) Site, L. D.; Alavi, A.; Lynden-Bell, R. M. *Mol. Phys.* **1999**, *96*, 1683.
 (55) Laaksonen, A.; Sprik, M.; Parrinello, M.; Car, R. *J. Chem. Phys.* **1993**, *99*, 9080.
 (56) Coulson, C. A.; Eisenberg, D. *Proc. R. Soc. London A* **1966**, *291*, 445.
 (57) Batista, E. R.; Xantheas, S. S.; Jónsson, H. *J. Chem. Phys.* **1998**, *109*, 4546.
 (58) Gregory, J. K.; Clary, D. C.; Liu, K.; Brown, M. G.; Saykally, R. J. *Science* **1997**, *275*, 814.
 (59) Kemp, D. D.; Gordon, M. S. *J. Phys. Chem. A* **2008**, *112*, 4885.
 (60) Tu, Y.; Laaksonen, A. *Chem. Phys. Lett.* **2000**, *329*, 283–288.

- (61) Abu-Samha, M.; Borve, K. J. *J. Chem. Phys.* **2008**, 128.
 (62) Ichikawa, K.; Kameda, Y.; Yamaguchi, T.; Wakita, H.; Misawa, M. *Mol. Phys.* **1991**, *73*, 79–86.